Capacitance-voltage measurements of hetero-layer OLEDs treated by an electric field and thermal annealing

Mohammed S. Al-Qrinawi[1,2], Taher M. El-Agez[1,2], Monzir S. Abdel-Latif[2,3] and Sofyan A. Taya[1,2,4],*

[1]*Physics Department, Islamic University of Gaza, Gaza, Palestine*
[2]*Renewable Energy Center, Islamic University of Gaza, Gaza, Palestine*
[3]*Chemistry Department, Islamic University of Gaza, Gaza, Palestine*
[4]*Department of Electrical and Computer Engineering, University of Waterloo, 200 University Avenue West, Waterloo, Ontario N2L 3G1, Canada*

Abstract: Capacitance-voltage (C-V) characterization of organic light-emitting diodes (OLEDs) having the structure ITO/ PVK (poly (9-Vinylcarbazole)/Rhodamine B dye/Pb is reported. The C-V curves provide more understanding about processes occurring in OLEDs like the voltages at which holes and electrons start flowing from the two electrodes through the OLED layers and the voltages at which emission starts. The OLEDs were fabricated under the same annealing conditions with an additional standard device without annealing for comparison. After depositing the Rhodamine B dye layer on the PVK thin film, samples were thermally annealed at different temperatures. The Pb layer was then deposited. Some samples were thermally annealed without applying any field, while others were annealed at the same temperatures under an external electric field. It was found that devices treated by only thermal annealing and those annealed under an electric field do not show any light emission whereas the standard device fabricated without any annealing does. The main difference between devices fabricated by exposure to an electric field while annealing and other devices is the lower turn-on voltages of the former devices.

Keywords: light-emitting diodes; PVK; Rhodamine B; temperature annealing; C-V curves.

1 Introduction

Organic light-emitting diodes (OLEDs) became very popular in recent years due to many advantages such as low cost, lightweight, better efficiency and large-area flat panel displays. An intensive effort was made to understand the operating mechanisms of OLED devices [1-6]. High work function material is a basic layer in the structure of an OLED. It has to be a transparent conducting layer to be used as an anode. A single organic layer or more is also needed as an emitting layer. A low work function layer is usually used as the cathode. Three key processes are responsible for light emission in an OLED: (i) injection of charge and transport, (ii) recombination of charges with energy transmission, and (iii) light production. Each of these procedures acts as an essential function in the turn-on voltage value, luminance and external efficiency of an OLED.

One of the efficient methods for studying material electrical properties and interfaces is impedance spectroscopy (IS). IS can be employed to understand the charge mobility in the interfacial regions or dynamics of the bound state. Moreover, it has the advantage of being a nondestructive technique. IS was also efficiently applied to a diversity of structures for electronic organic devices [7]. In 2005, Y. Yang and V. Shrotriya examined several metals as cathodes, like gold (Au), Aluminum (Al) and calcium (Ca), to investigate the effect of injection of charge on the capacitance-voltage properties [5]. The impact of heat and electric field treatments on polymer light-emitting diodes (PLEDs) was investigated by S. Mutlu and A. Osman [6] where they observed an increase in the turn-on voltage. Also, they

*Corresponding author E-mail: philominathan@gmail.com

concluded that treatment by heat restores the light-emitting function of dysfunctional PLEDs [6]. S. Nowy et al. employed IS technique to study the injection properties of charge carriers from different anodes and anode treatments in bottom-emitting OLEDs [7].

The impact of post-fabrication thermal annealing with and without an external electric field on OLEDs is reported in this work. The C-V characteristics of the fabricated OLEDs are also investigated. We relate the behavior of C-V curves to the onset of majority and minority charge carrier injection from the electrodes into the active organic layer.

2 Experimental Section

2.1. Fabrication

All fabrication steps are implemented at 26ºC. The substrate material is taken as ITO. The sheets of ITO are cut into squares of dimensions of 2.5 cm × 2.5 cm and are employed as anodes. ITO squares were cleaned in an ultrasonic bath using isopropanol and acetone and dilute aqua regia solution. The concentration of aqua regia solution was a diluted solution of 3:1 concentrated HCl:HNO$_3$ mixture at a temperature of 60 ºC for 5 min. They are then washed by distilled water in an ultrasonic cleaner for 20 min and placed in an oven at 60°C.

After careful cleaning of ITO surface, the PVK layer was deposited on ITO surface. An amount of PVK powder (15 mg) was dissolved in a mixture of solvents containing 1 ml toluene and 5 ml tetrahydrofuran (THF). After obtaining a homogenous solution, it was deposited on the ITO surface to form a thin film. The film thickness was measured using Filmetrics (F20-UVX) and found to be 45 nm. The PVK film was obtained by placing a little of the homogeneous solution on the ITO substrate surface. The samples were maintained in an inclined position of 45° for several minutes to allow the solution to spread on the surface and form a thin film on PVK. This method is one of the commonly used techniques to prepare thin films which is considered of high sensitivity to the temperature differences due to different evaporation rates of solvents [8].

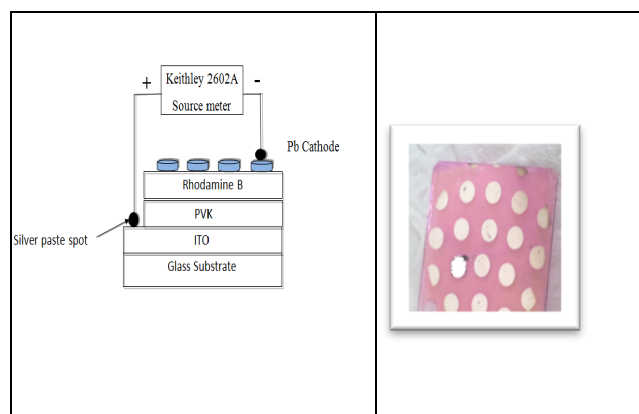The fabricated devices have the form ITO/PVK/Rhodamine B/Pb as plotted in Fig. 1.

Fig. 1. The pictures on the left and right show a schematic diagram of a double-layer OLED (ITO/PVK/Rhodamine B/Pb) and the OLED device after fabrication, respectively.

2.2. Post-processing treatment

A vacuum deposition technique was used to deposit Rhodamine B dye on the PVK surface. By heating a source of Rhodamine B dye under vacuum, it evaporates or sublimes into a gaseous vapor. The vapors condense on the PVK surface to form a thin film. The thickness of the deposited film is determined using a quartz crystal monitor. After adding the Rhodamine B dye above the PVK layer, samples were thermally annealed at different temperatures of 90ºC, 100ºC, 110ºC and 120ºC. The annealing time was conducted for 15 min and was the same for all samples, using a hot plate under the atmospheric environment. Finally, the Pb cathode film was deposited on the top of the Rhodamine B dye layer by thermal vacuum evaporation. Some samples were heat-treated without applying an electric field while others were annealed under an external electric field. Exposing to an electric field was done in the following manner. While being thermally annealed, some of the samples were exposed to a +10 KV voltage applied to Cu-disc with a diameter of 5 cm placed 2 cm above the device while the ITO electrode was grounded. The hot plate was

stopped while applying the electric field for an extra 15 min. After that, the electric field was turned off. As a final step in the fabrication method, a 35 nm Pb film was thermally vacuum evaporated on the top of the organic layer as a second electrode. The setup of the electric field is shown in Fig. 2
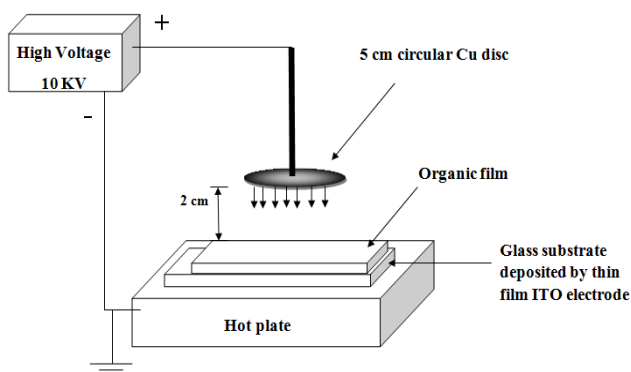

Fig. 2. *The electric field setup treatment.*

3 Results and Discussion

Figure 3 illustrates four different regions into a typical OLED C-V. The four regions are neutral, dark current, majority charge-injection, and charge recombination regimes. A bias voltage (V_1) is the applied voltage at which the injection of the majority charge into the organic layer starts in forward bias [5]. For $V < V_1$, the organic layer is neutral. There is a small quantity of charge trapped near the interface. The organic layer is thought of as composed of large neutral region and small charge regions at the interface [5]. For $V > V_1$, a sharp capacitance growth can be noticed due to the injection of the majority charge. The voltage V_2 is the applied bias at which the radiation emission from the device starts. This voltage marks a sharp decay in the device capacitance value [5]. Voltage V_2 sometimes called built-in value (V_{bi}) which is the voltage at *which the minority charge begins* injection into the organic layer. Figure 4 illustrates the C-V curve of the control OLED device with the construction of (ITO/44.88 nm PVK/30.00 nm

Rhodamine B dye/35.00 nm Pb). The C-V characteristic curve displays main and secondary peaks which refer to the charge injection into the device [5]. At the first secondary peak, the capacitance raises at a transition voltage V_{T1} which has a value of about 7.0 V since holes begin injection into the device. At a voltage of 7.7 V, some electrons can be injected from the cathode, which is called built-in voltage V_{bi1}. With further increase of the applied voltage, the capacitance decreases until the transition voltage V_{T2} of about 8.6 V which is considered the main peak at which holes had injected into the PVK layer. For $V_{bi2} = 9.7$ V, electrons had injected from the cathode into the OLED device. Consequently, the charge is annihilated due to holes and electrons recombination generating emitted light.
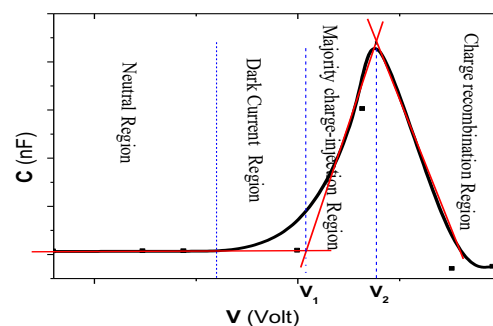

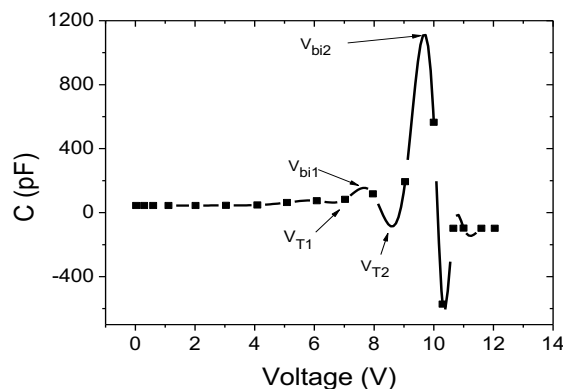**Fig. 3.** Ideal C-V characteristic curve for an OLED.

Fig. 4. C-V curve of the control device consisting of (ITO/45nm PVK/30nm Rhodamine B/ 35nm Pb). It was fabricated without any annealing.

Figure 5 shows the C-V curves for devices treated at different temperatures without an electric field. Minor and major peaks can be noticed in the C-V curves. These peaks indicate that the flow of charges through the device occurs in several stages. The holes are injected into the device when the bias exceeds transition voltages V_{T1} or V_{T2}, leading to a rise in the capacitance due to the accumulation of charges at the barriers. When the bias reaches the built-in voltages V_{bi1} or V_{bi2}, bipolar charge carriers start the injection. When the bias becomes greater than V_{bi1} or V_{bi2}, capacitance starts to decrease because of the recombination of holes and electrons. As the temperature increases, the transition and built-in voltages are enhanced as shown in Table 1 except at a temperature of 100 $^\circ$C. This result is similar to that obtained in reference [9,10].

The C-V curves for devices exposed to an electric field during the thermal annealing are shown in Fig. 6. As can be seen, main and minor peaks are noticed which indicate the charge injection into the OLED device. Table 2 presents the values of transition and built-in voltages for all devices. The advantage of exposing devices to an electric field after the heat annealing improves the performance of devices by reducing their turn-on voltages. Moreover, it improves their photovoltaic function by increasing their short circuit currents and open-circuit voltages.
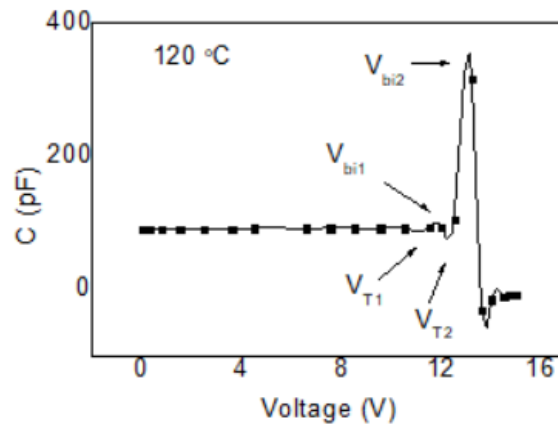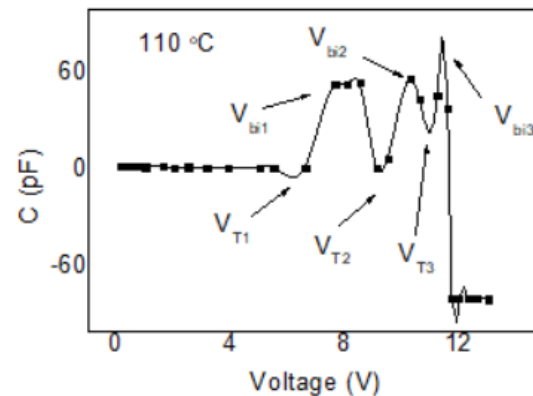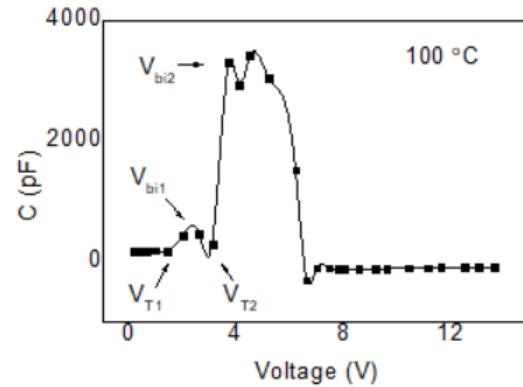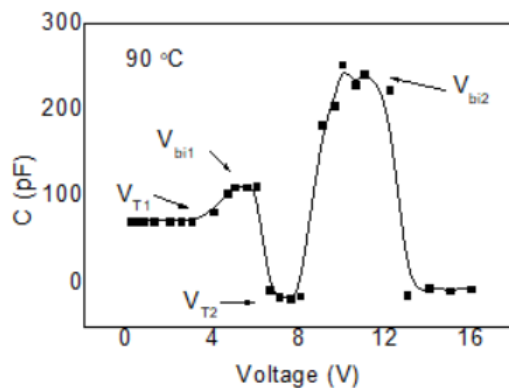

Fig. 5. C-V curves for devices containing of (ITO/45nmPVK/30nm Rhodamine B dye/35nm Pb) at different annealing temperatures.

Table 1. The build-in and transition voltages for various annealing temperatures.

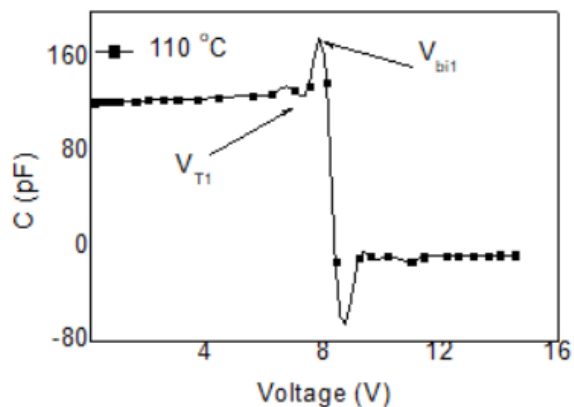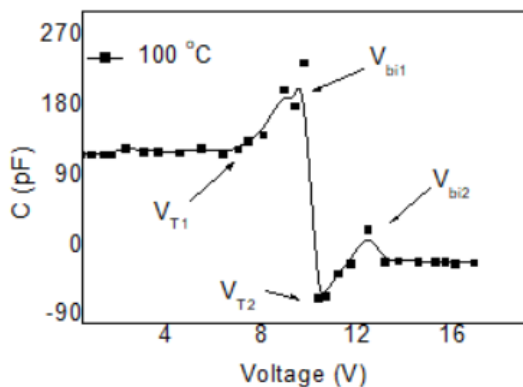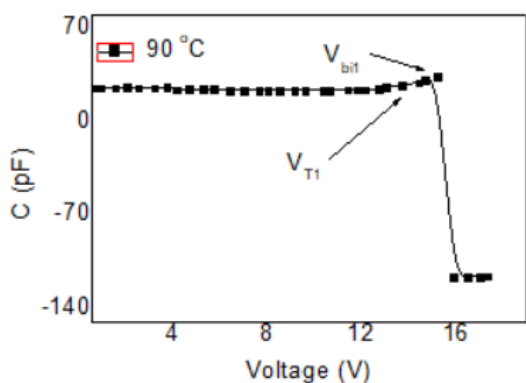| Temperature	Standard device	90℃	100℃	110℃	120℃
V_{T1}	7.0	3.0	1.5	6.6	11.5
V_{T2}	8.6	8.0	3.0	9.3	12.3
V_{T3}	……	…..	…..	11.0	…..
V_{bi1}	7.7	5.5	2.3	8.0	11.7
V_{bi2}	9.7	11.0	4.6	10.3	13.0
V_{bi3}	…..	…..	…..	11.5	…..
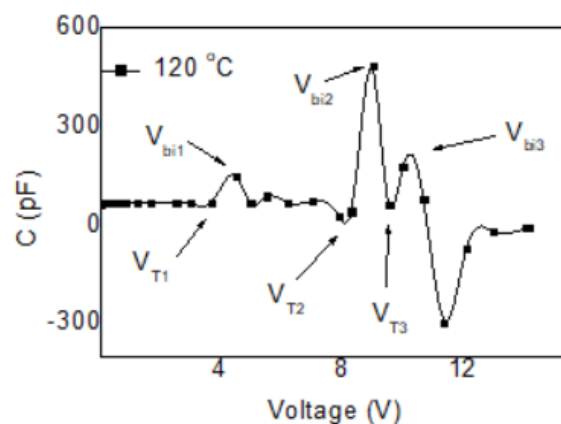
Fig. 6. Capacitance-voltage curves for devices containing of (ITO/45nm PVK/30nm Rhodamine B dye/35nm Pb) which were treated by an external electric field at different annealing temperatures.

Table 2. Transition and build-in voltages for OLED devices treated by an electric field through thermal annealing.

Temperature	Standard device	90℃	100℃	110℃	120℃
V_{T1}	7.0	13.2	7.0	7.3	3.7
V_{T2}	8.6	…..	10.5	…..	8.2
V_{T3}	……	…..	…..	…..	9.6
V_{bi1}	7.7	14.8	9.4	7.8	4.3
V_{bi2}	9.7	…..	12.5	…..	8.9
V_{bi3}	…..	…..	…..	…..	10.2

The C-V curves for all OLED devices treated by annealing with and without an E-field are shown in Fig. 7. It is clear that the C-values of devices treated by an E-field at temperatures of 90℃ and 100℃ were smaller than those of the devices treated by thermal annealing only at the same temperatures. However, devices treated with an E-field at temperatures of 110℃ and 120℃ are found to have higher capacitances than those treated by thermal annealing only at the same temperatures. It is expected that the electric field at temperatures of 110℃ and 120℃ attracts the dye from the edges of the device and makes dye aggregation as shown in Fig. 8. As a result, the luminance disappeared and this result is in agreement with that obtained in reference [11]. Figure 9 shows the reflected beam received from the sample center and the two edges which was treated by an electric field at a temperature 110℃. There is an obvious difference between the reflected beam from the center of the sample and those reflected from the edges.
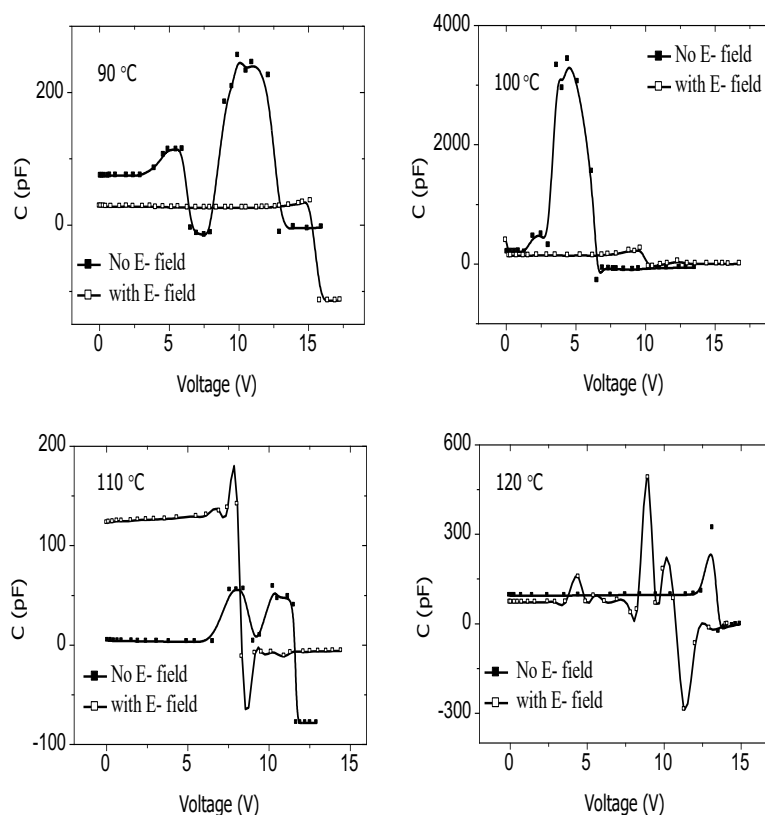

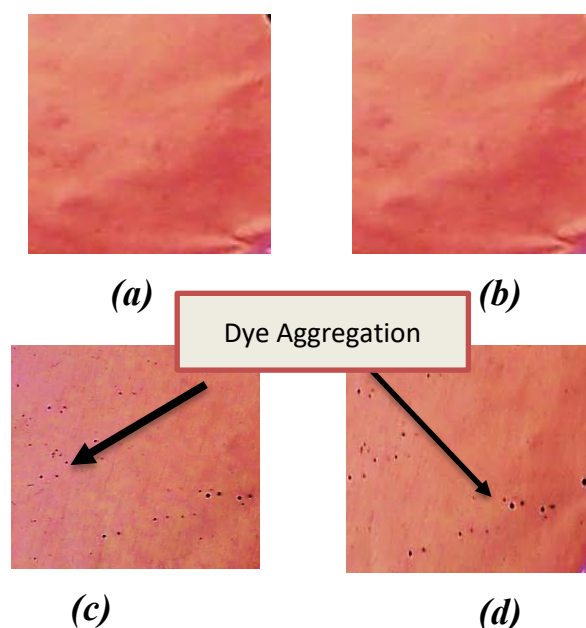**Fig. 7.** C-V curves for devices containing treated by heat only and heat with an electric field.

Fig. 8. Photos of samples treated by an external electric field at temperature 90℃ (a), 100℃ (b), 110℃ (c) and 120℃ (d).
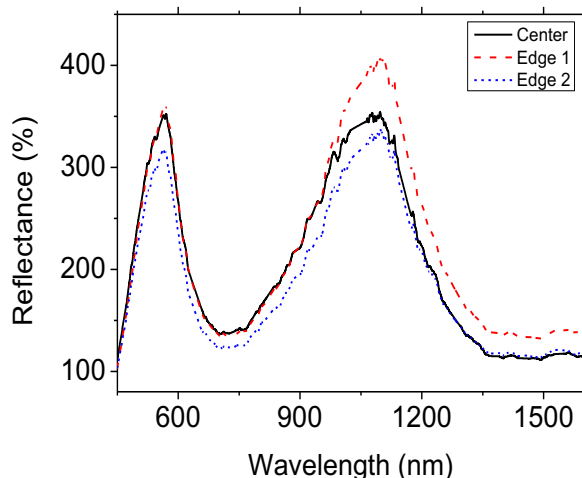
Fig. 9. The reflected beam received from the sample center and the two edges. The sample was treated by an electric field at temperature $110^{\circ}C$.

Figures 10 through 12 show the current density-capacitance and luminesces-capacitance curves as functions of the applied forward bias for all devices. It is clear that, when the capacitance starts to rise in the C-V curve, the current density also rises in the J-V curve almost at the same voltage. In addition, the light emission from the control device is detected at a similar value of the applied potential at which the capacitance begins declining. Sometimes, the experimental values of the voltage at which the device starts emission (V_{on}) can change to turn-on and built-in voltages by a few tenths of a volt as obviously shown in Figs. 10(a) and 10(b) [6]. The current density and light intensity-capacitance curves are shown as a function of the applied forward bias of the device consisting of (ITO/PVK/Rhodamine B/Pb) [3]. Figures 11 and 12 show the J-V and C-V curves for devices treated at different temperatures (Fig. 11) and those exposed to an electric field during thermal annealing (Fig. 12). As shown in the two figures, at V_T in the C-V curves at which the major charges are injected into the devices, the current density begins to increase in the J-V curves. At built-in voltages in the C-V curves, the minor charges are injected from the electrode into the device. With a further increase of the potential, the capacitance of the devices declines rapidly as electrons and holes recombine to each other.

Furthermore, the current density significantly increases because more holes and electrons are injected into the devices from the two electrodes.
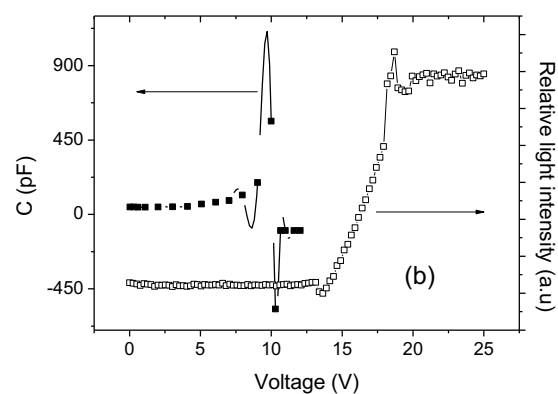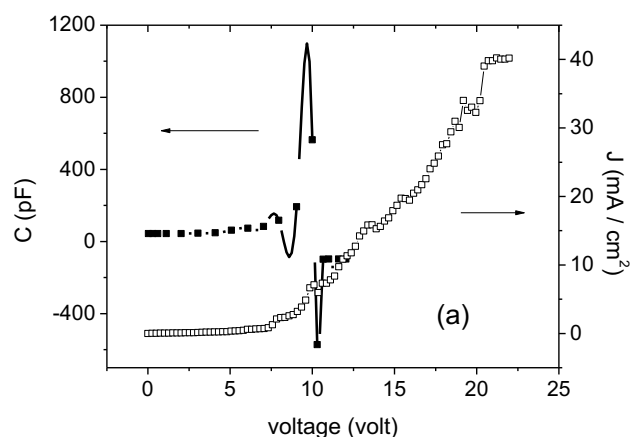

Fig. 10. Capacitance and current density curves as functions V (a), and capacitance with relative light intensity as functions V (b) for the control device containing of (ITO/45nm PVK/30nm Rhodamine B/35nm Pb) device.
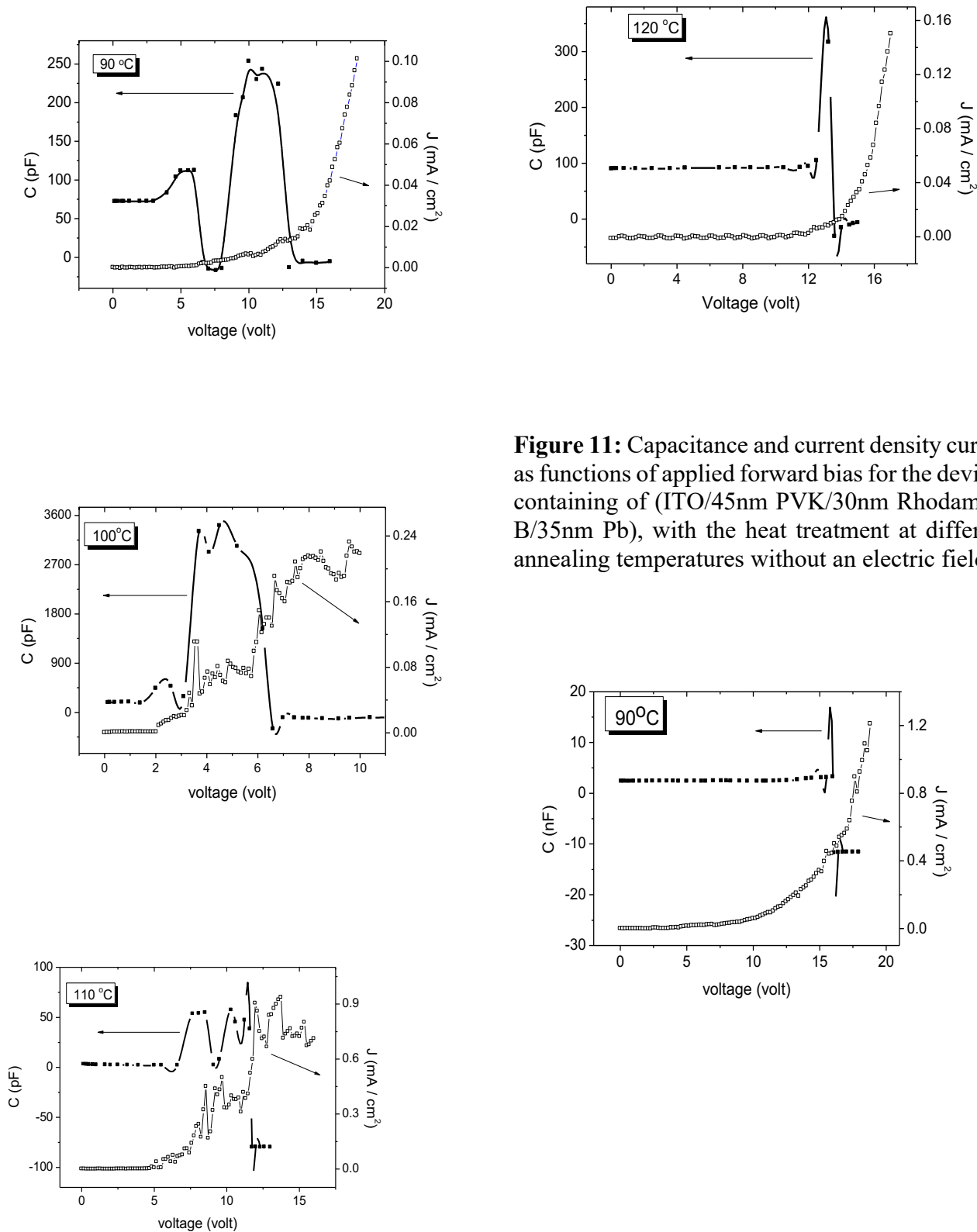
Figure 11: Capacitance and current density curves as functions of applied forward bias for the devices containing of (ITO/45nm PVK/30nm Rhodamine B/35nm Pb), with the heat treatment at different annealing temperatures without an electric field.
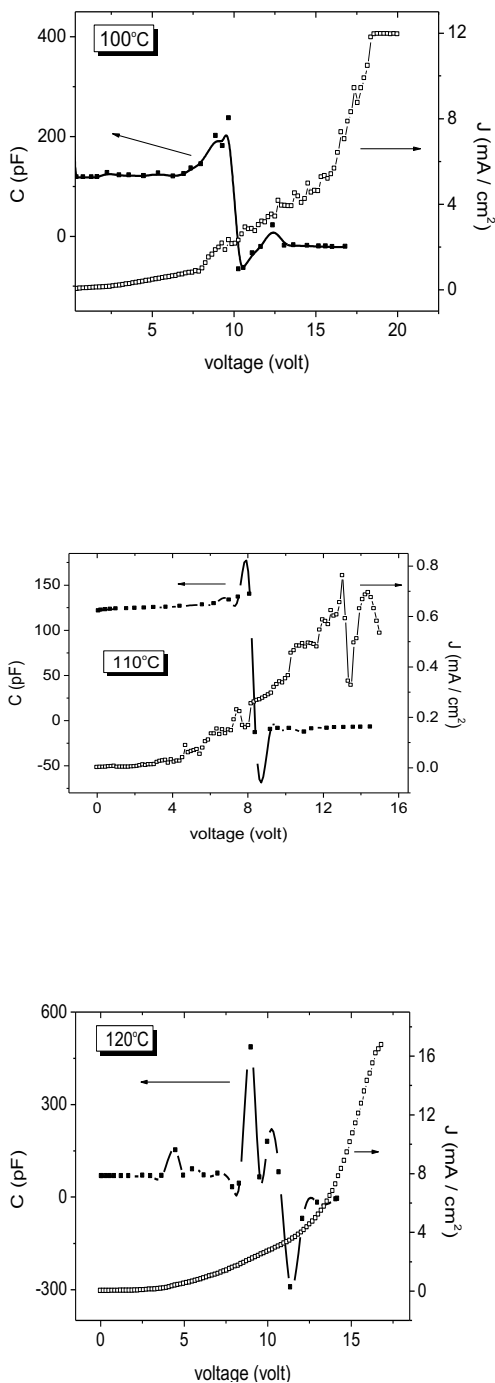
Figure 12: Capacitance and current density curves as functions of applied forward bias for device containing of (ITO/45nm PVK/30nm Rhodamine B/35nm Pb), with an electric field during heating.

4 Conclusions

We have used the technique of impedance spectroscopy to analyze the injection of charges in an OLED device. The structure of the tested OLED was (ITO/ PVK/Rhodamine B dye/Pb). All devices have constructed in the same way along with the control device. The reference device was fabricated without annealing to compare with other devices. All fabricated devices either treated by heating or by an electric field through heating were not observed to emit light compared to the control device. Lack of light emission from these devices can be attributed to the dye aggregation as suggested by the literature but may need further investigation. The electric field at temperatures of 110 ºC and 120 ºC attracts the dye from the edges to the center. On the other hand, the best annealing temperature in the presence of an electric field was 120 ºC which corresponds to the highest current density. This work suggests that capacitance-voltage analysis can be used as a sensitive technique to observe the injection of charge better than current density-voltage measurements.

References

[1] S. Berleb, W. Brutting, G. Paasch, "Interfacial charges in organic hetro-layer light emitting diodes probed by capacitance-voltage measurements", Synthetic Metals 122 (2001) 37-39.
[2] V. Shrotriya and Y. Yang. "Capacitance-voltage characterization of polymer light-emitting diodes", Journal of applied physics 97, 054504 (2005).
[3] S. Nowy, W. Ren, J. Wagner, J. Weber, and W. Brutting, "Impedance spectroscopy of organic hetro-layer OLEDs as a probe for charge carrier injection and device degradation", Proc. of SPIE Vol. 7415, 74150G-1 (2009).
[4] P. Kao, S. Chu, S. Liu, Z. You, C. Chuang, Improved performance of organic light-emitting diode using a metal-phthalocyanine hole-injection layer, Journal of the electrochemical society **153** (2006) 122-126
[5] V. Shrotriya, Y. Yang, Capacitance-voltage characterization of polymer light-emitting diodes, Journal of applied physics **97** (2005) 054504.
[6] A. Osman and S. Mutlu, "Post-fabrication electric field and thermal treatment of polymer light emitting diodes and their photovoltaic properties", Organic Electronics 10 (2009) 18-26.
[7] S. Nowy, W. Ren, J. Wagner, J. Weber, W. Brutting, Impedance spectroscopy of organic hetro-layer OLEDs as a probe for charge carrier injection and device degradation, Proc. Of SPIE **7415** (2009).
[8] El-Agez, T., Taya, S., Tayyan, A., Abdel-Latif, M. & Afghjani, A. (2013). Electroluminescence from Single PVK Layer Organic Light Emitting Diode Using Different Dyes at Different Concentrations, Physical Review & Research International, 3, 306-320.
[9] Z. Chunlin, Z. Yong, L. Haixia, W. Fangcong, Z. Guobing, C. Da, J. Xiaoyun and L. Su, "Enhancing the Performance of the Organic Light-Emitting Device (OLED) by Thermal Treatment", Chinese Journal of Electronics, Vol. 20, No.1, Jan.2011.
[10] S. Jang, H. Chae, D. Jung, H. Kim, Ch. Kim, "Simultaneous Oxygen Plasma and Thermal Treatments of an ITO Surface to Improve the Electrical Characteristics of Organic Light-Emitting Diodes", Journal of the Korean Physical Society, Vol. 51, No. 3, September 2007, pp. 956_962.
[11] B. Chen, X. Sun and K. Sarma, "Phosphorescent organic light-emitting device with in situ post-growth annealed organic layers", Material Science and Engineering B, 139(2007), 192-196.